Received March 2003
Revised August 2003
Accepted September 2003

Numerical study of turbulent boundary layers with heat transfer and tangential transpiration

Burhan Çuhadaroğlu
Department of Mechanical Engineering, Karadeniz Technical University, Trabzon, Turkey

Keywords *Heat transfer, Porous materials, Boundary layers, Numerical analysis*

Abstract *The hydrodynamic and thermal characteristics of the turbulent boundary layer developed on a porous wall with heat transfer and various angles of transpiration are analyzed numerically with the proper boundary conditions. The wall functions of the viscous and turbulent sub-layers for velocity and temperature are modified to allow for the effect of the angle of injection and suction through the porous wall. The finite difference method based on a control volume approach is used for solving the time averaged Navier-Stokes equations for incompressible flow in conjunction with the standard k-ε turbulence model equations. A non-uniform staggered grid arrangement is used. The parameters studied include the suction and injection velocity (V_w) and the angle (α) of the injection and suction. The present numerical results of the normal injection and suction are compared with a known experimental data and a good agreement is obtained. The numerical results also indicate that the characteristics of the turbulent boundary layer such as local friction coefficient and thermal boundary layer thickness are substantially influenced by the velocity and the angle of transpiration.*

Nomenclature

C_f = local friction coefficient
C_μ, C_1, C_2, σ_k, σ_ε = turbulence model constants
I,J = value at (i, j) cell
I_{MAX}, J_{MAX} = maximum values of grid numbers
k = turbulence kinetic energy
n = normal direction to the porous wall
p = pressure
Pr = Prandtl number, $\mu C_p/\lambda$
Pr_t = turbulent Prandtl number
Re = Reynolds number based on porous wall length, $U_\infty X_L/\nu$
r = mesh expansion ratio
T = temperature
Tu = turbulence intensity, $Tu = 100\left[\frac{1}{3}\left(\overline{u'^2}+\overline{v'^2}+\overline{w'^2}\right)\right]^{1/2}/U_\infty$
U, V = velocity components
U_τ = friction velocity
V_w = injection and suction velocity
X_L, Y_L = horizontal and vertical lengths of the computation domain
x, y = Cartesian coordinates

Greek symbols
α = angle of injection and suction
ε = turbulence energy dissipation rate
$\Delta x, \Delta y$ = distances between the grid points
δ_{ij} = kronecker delta
δ_T = thermal boundary layer thickness
ϕ = any dependent variable (i.e. U, k, T)
κ = von Karman constant ($\kappa = 0.4$)
λ = thermal conductivity

This work was financially supported by Karadeniz Technical University Research Fund.

International Journal of Numerical Methods for Heat & Fluid Flow
Vol. 14 No. 6, 2004
pp. 760-782

0961-5539
DOI 10.1108/09615530410544300

μ	= dynamic viscosity	t	= turbulent
ρ	= density	w	= wall
υ	= kinematic viscosity	∞	= free stream

Subscripts

eff	= effective
p	= intersection point of sub-layers
pT	= intersection point of thermal sub-layers

Superscripts

+	= normalized quantity
$'$	= fluctuating quantity
$-$	= time average

Introduction

The wall transpiration as a boundary layer control technique is a frequently encountered application in thermal fluids engineering. The main aim of this artifice is to add momentum and heat to the flow so that it can be made to conform to some desired parameter. For instance, injection from a porous wall causes to thicken boundary layer and also to decrease surface skin friction and hence the drag decreases. Injection is also an effective tool to produce film cooling for high speed systems which are exposed to high temperatures such as nozzle of spacecraft engines and turbine blades. Suction is frequently used to delay or avoid the boundary layer separation and to prevent the transition to turbulence. Even though the magnitude of the transpiration rate is often low compared with the mainstream, it significantly changes the surface skin friction as well as the turbulence quantities near the wall.

A general study on turbulent boundary layer with heat transfer and transpiration through a porous wall has three basic compounds:

(1) turbulent constitution of boundary layer developed on porous wall;

(2) heat transfer between flow and porous wall; and

(3) analysis technique such as experimental and computational.

Effects of transpiration velocity on turbulent flow parameters, such as mean velocity and temperatures profiles, the skin-friction coefficient and also the convective heat transfer coefficient, have been studied in great detail in the literature. Simpson (1970) reviewed the existing works on turbulent boundary layers with and without normal transpiration, and also extended the law of the wall of the wake formulation to the cases with transpiration. Schetz and Nerney (1977) experimentally investigated the turbulent boundary layer with normal injection and surface roughness. The results of this study reveals that the velocity and turbulence intensity in the turbulent boundary layer increased with increasing rate of injection. The perturbation methods were applied to the problem of transpired turbulent boundary layers and it was also obtained the bilogarithmic laws for the wall and defect layers through the perturbation method by Silva Freire (1988). The study of the topology of a turbulent boundary layer with and without wall suction was carried out by Antonia and Fulachier (1989). The effect of uniform normal mass bleed into the separated-reattaching flow over a backstep was investigated experimentally by Yang *et al.* (1994). Antonia and Zhu (1995) investigated the relaminarization of turbulent boundary layer with suction through a slot by measuring the wall shear stress, the mean velocity and the main Reynolds stresses. The analytical treatment of problems that combine compressibility

effects, transfer of heat and transpiration were carried out by Silva Freire *et al.* (1995). The integral form of the momentum equation of transpired turbulent boundary layer with pressure gradient was numerically solved and predicted the variations of the skin friction coefficient and integral thickness with distance by Sucec and Oljaca (1995). Bellettre *et al.* (1999) numerically investigated a turbulent boundary layer submitted to injection through a porous plate and compared the results obtained with experimental measurements. Avelino *et al.* (1999) used an analytical approach to obtain wall functions for transpired turbulent boundary layers. Hwang and Lin (2000) predicted the dynamic and thermal fields in flows with transpiration by adopting an improved low Reynolds number k-ε model and the direct numerical simulation (DNS). Djenidi and Antonia (2001) investigated the effect of concentrated suction through a porous wall strip on a turbulent boundary using a turbulence model, based on a second-order moment closure.

Near wall modeling of turbulent heat fluxes with second moment closure was carried out by Lai and So (1990). The closure results of this study show that the turbulent Prandtl number is not constant in the near wall region. Antonia and Kim (1991), using the near wall DNS data for the Reynolds shear stress and heat flux, showed that the wall value of turbulent Prandtl number is about 1.1. So *et al.* (2000) investigated the effects of five different near-wall Reynolds-stress models on the calculated thermal field in an incompressible flow. The results of this study reveal that the calculated mean temperature is very sensitive to the near-wall Reynolds-stress model used to evaluate the velocity field.

Although the turbulent boundary layer on a porous wall with normal transpiration has been studied by many investigators, the effects of the tangential transpiration on the hydrodynamic and thermal characteristics of boundary layer have not been studied in detail. As is known well, transpiration alters the structure of the turbulent boundary layer rather considerably, affecting the shear-stress distribution, and also strongly affecting the sub-layer thickness (Kays and Crawford, 1980). Here, "tangential" is added to transpiration and using the modified wall laws of velocity and temperature include the tangential transpiration effects, numerical aspect of a turbulent boundary layer submitted to tangential transpiration is analyzed. The numerical results of uniform normal injection are compared with the experimental measurements given by Bellettre *et al.* (1999) and the agreement is found to be satisfactory.

Formulation

The governing equations

The Reynolds-averaged continuity, Navier-Stokes and temperature equations can be written as:

$$\frac{\partial U_j}{\partial x_j} = 0 \tag{1}$$

$$\frac{\partial(\rho U_i U_j)}{\partial x_j} = -\frac{\partial p}{\partial x_i} + \frac{\partial}{\partial x_j}\left[\mu\left(\frac{\partial U_i}{\partial x_j} + \frac{\partial U_j}{\partial x_i}\right) - \rho\overline{u_i' u_j'}\right] \tag{2}$$

$$\frac{\partial(\rho U_j T)}{\partial x_j} = \frac{\partial}{\partial x_j}\left[\frac{\mu}{\mathrm{Pr}}\frac{\partial T}{\partial x_j} - \rho\overline{u_j' T'}\right] \tag{3}$$

where U, T and P are the mean values of velocity, temperature and pressure, ρ the fluid density, μ the dynamic viscosity and Pr the Prandtl number. In these equations, μ and Pr are temperature dependent and ρ follows the ideal gas law.

Within the framework of an eddy viscosity and adopting the Boussinesq approximation, the Reynolds stress and heat flux are approximated as:

$$-\overline{u_i' u_j'} = \upsilon_t\left(\frac{\partial U_i}{\partial x_j} + \frac{\partial U_j}{\partial x_i}\right) - \frac{2}{3}\delta_{ij}k \tag{4}$$

$$-\overline{u_j' T'} = \frac{\upsilon_t}{\mathrm{Pr}_t}\frac{\partial T}{\partial x_j} \tag{5}$$

where υ_t and Pr_t are the turbulent kinematic viscosity and Prandtl number (chosen as 1.0 near the wall), respectively. In the present study, the standard k-ε turbulence model is used which allows to analyze the flows with high Reynolds number. The model equations are:

$$\frac{\partial(\rho U_j k)}{\partial x_j} = \frac{\partial}{\partial x_j}\left(\frac{\mu_{\mathrm{eff}}}{\sigma_k}\frac{\partial k}{\partial x_j}\right) + \mu_{\mathrm{eff}}\left(\frac{\partial U_i}{\partial x_j} + \frac{\partial U_j}{\partial x_i}\right)\frac{\partial U_i}{\partial x_j} - \rho\varepsilon \tag{6}$$

$$\frac{\partial(\rho U_j \varepsilon)}{\partial x_j} = \frac{\partial}{\partial x_j}\left(\frac{\mu_{\mathrm{eff}}}{\sigma_\varepsilon}\frac{\partial \varepsilon}{\partial x_j}\right) + C_1\frac{\varepsilon}{k}\mu_{\mathrm{eff}}\left(\frac{\partial U_i}{\partial x_j} + \frac{\partial U_j}{\partial x_i}\right)\frac{\partial U_i}{\partial x_j} - C_2\rho\frac{\varepsilon^2}{k} \tag{7}$$

$$\mu_{\mathrm{eff}} = \mu + \mu_t \tag{8}$$

$$\mu_t = \rho C_\mu k^2/\varepsilon \tag{9}$$

with $\sigma_k = 1.0$, $\sigma_\varepsilon = 1.3$, $C_1 = 1.44$, $C_2 = 1.92$ and $C_\mu = 0.09$.

Boundary conditions

At the inflow boundary of the computation domain uniform velocity profile imposed with:

$$U = U_\infty, \quad k = 1.5(\mathrm{Tu}U_\infty)^2, \quad \varepsilon = C_\mu^{3/4}k^{3/2}/\kappa y, \quad T = T_\infty \tag{10}$$

Along the outflow and free boundaries where the flow field is regarded as fully developed, the normal derivatives of all properties are zero, i.e. (Figure 1)

$$\frac{\partial U}{\partial n} = 0, \quad \frac{\partial V}{\partial n} = 0, \quad \frac{\partial k}{\partial n} = 0, \quad \frac{\partial \varepsilon}{\partial n} = 0, \quad \frac{\partial T}{\partial n} = 0 \tag{11}$$

In the near-porous wall region, which has two sub-layers, two different formulas have been used in computational algorithm (Çuhadaroğlu, 2001). The viscous sub-layer was simulated as:

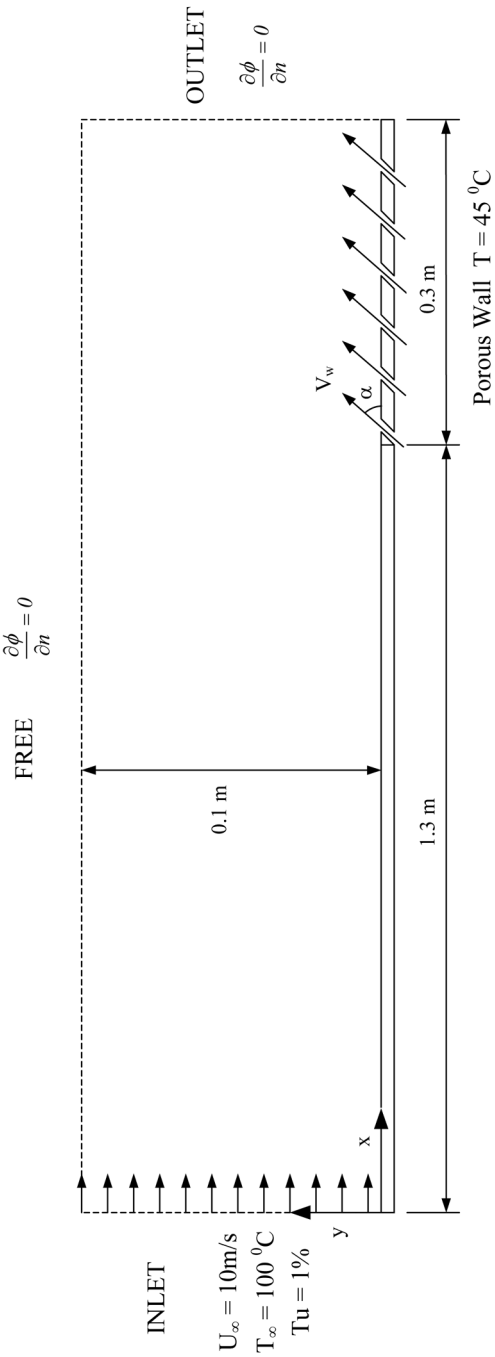

Figure 1.
The schematic representation of the flow field and the boundaries

$$U^+ = \frac{\exp\left(y^+ V_{\mathrm{w}}^+ \sin\alpha\right) + \left(V_w^{+2} \sin 2\alpha\right)\Big/2 - 1}{V_{\mathrm{w}}^+ \sin\alpha} \tag{12}$$

and in the turbulent sub-layer

$$U^+ = \frac{V_{\mathrm{w}}^+ \sin\alpha}{4\kappa^2}\left[\ln\left|\frac{y^+}{y_{\mathrm{p}}^+}\right|\right]^2 + \frac{1}{\kappa}\ln\left|\frac{y^+}{y_{\mathrm{p}}^+}\right| \times\left[1 + U_{\mathrm{p}}^+ V_{\mathrm{w}}^+ \sin\alpha - \left(V_{\mathrm{w}}^{+2}\sin 2\alpha\right)\Big/2\right]^{1/2} + U_{\mathrm{p}}^+ \tag{13}$$

has been regarded with the constants of $U_p^+ = y_p^+ = 11.5$ and $\kappa = 0.4$ (Çuhadaroğlu, 2001). Finally, the wall functions used in this study can be summarized as follows:

$$U^+ = \left\{\begin{array}{ll} \text{Equation (12);} & \text{for } y^+ < y_{\mathrm{p}}^+ \\ \text{Equation (13);} & \text{for } y^+ \geq y_{\mathrm{p}}^+ \end{array}\right\} \tag{14}$$

In the vicinity of the wall, the turbulent sublayer is in local equilibrium so that the rate of turbulence kinetic energy production is exactly equal to its dissipation rate ($G = \rho\varepsilon$). Therefore, at the point close to the porous wall, the value of turbulence kinetic energy k is calculated solving the transport equation of turbulence kinetic energy neglecting the production and dissipation terms, while the energy dissipation ε can be evaluated by the expression

$$\varepsilon = \frac{C_\mu^{3/4} k^{3/2}}{\kappa y} \tag{15}$$

As is known well, the effect of transpiration on the turbulent thermal boundary layer is very similar to the effect on the hydrodynamic boundary layer. The temperature equation of two-dimensional incompressible turbulent boundary layer with constant temperature along the porous wall can be regarded as

$$V\frac{\mathrm{d}T}{\mathrm{d}y} = \frac{\mathrm{d}}{\mathrm{d}y}\left(\frac{k}{\rho C_{\mathrm{p}}}\frac{\mathrm{d}T}{\mathrm{d}y} - \overline{v'T'}\right) \tag{16}$$

Integrating equation (16) from $y = 0$ to any y and using the porous wall conditions with tangential injection,

$$T\big|_{y=0} = T_{\mathrm{w}}, \quad k(\mathrm{d}T/\mathrm{d}y)\big|_{y=0} = q_w$$

and

$$\overline{v'T'}\big|_{y=0} = 0 \quad \text{at } y = 0$$

$$(T - T_{\mathrm{w}})V_{\mathrm{w}}\sin\alpha + \frac{q_{\mathrm{w}}}{\rho C_{\mathrm{p}}} = \left(\frac{\nu}{\mathrm{Pr}} + \frac{\nu_{\mathrm{t}}}{\mathrm{Pr}_{\mathrm{t}}}\right)\frac{\mathrm{d}T}{\mathrm{d}y} \tag{17}$$

where

$$\frac{\nu_t}{\mathrm{Pr}_t}\frac{\mathrm{d}T}{\mathrm{d}y} = -\overline{u_j' T'}\Big|_{y=y}.$$

Rearranging this equation we obtain

$$\frac{\mathrm{d}T}{\mathrm{d}y} = \frac{(T - T_w)V_w \sin\alpha + q_w/(\rho C_p)}{\frac{\nu}{\mathrm{Pr}} + \frac{\nu_t}{\mathrm{Pr}_t}} \tag{18}$$

In terms of normalized quantities, dimensionless temperature gradient equation can be written as

$$\frac{\mathrm{d}T^+}{\mathrm{d}y^+} = \frac{1 + T^+ V_w^+ \sin\alpha}{\frac{1}{\mathrm{Pr}} + \frac{\nu_t}{\nu \mathrm{Pr}_t}} \tag{19}$$

where the normalized temperature is defined as

$$T^+ = \frac{T - T_w}{q_w/(\rho C_p U_\tau)}. \tag{20}$$

Equation (19) gives the temperature gradient in turbulent boundary layer. Let us consider a two-layer model with a viscous sub-layer and a turbulent sub-layer as is done for hydrodynamic boundary layer. Neglecting the term $\nu_t/(\nu \mathrm{Pr}_t)$ and integrating it from the wall to an arbitrary non-dimensional coordinate gives wall function of viscous sub-layer for temperature as

$$T^+ = \frac{\exp(\mathrm{Pr}\, y^+ V_w^+ \sin\alpha) - 1}{V_w^+ \sin\alpha} \tag{21}$$

In turbulent sub-layer; the term 1/Pr can be neglected in equation (19). Using the mixing length formula for turbulent kinematic viscosity and integrating it from the point "pT" at which the viscous and turbulent thermal sub-layers intersect to any y^+, the wall function of turbulent sub-layer for temperature is obtained as

$$T^+ = \frac{1}{V_w^+ \sin\alpha}\left\{\left(1 + V_w^+ T_{pT}^+ \sin\alpha\right)\left[\frac{1 + U^+ V_w^+ \sin\alpha - \left(V_w^{+2} \sin 2\alpha\right)/2}{1 + U_{pT}^+ V_w^+ \sin\alpha - \left(V_w^{+2} \sin 2\alpha\right)/2}\right]^{\mathrm{Pr}_t} - 1\right\} \tag{22}$$

This equation defines an explicit relation between T^+ and U^+ which was used instead of a relation $T^+ = f(y^+)$. Equation (22) proves superior to $T^+ = f(y^+)$ for the flows have complex geometry. The values of T_{pT}^+ and U_{pT}^+ are determined from the wall function of viscous sub-layer without transpiration as $T_{pT}^+ = \mathrm{Pr}\, y_{pT}^+$ and $U_{pT}^+ = y_{pT}^+$ for $y_{pT}^+ = 13.2$ (Kays and Crawford, 1980).

Method of solution

The method of numerical solution used in this study is based on solving the set of discretization equations iteratively using a point by point method. The discretization

equations are derived by integrating the differential equations over a defined control volume. As is done in general, the calculation domain is discretized with a staggered grid which allows the prediction of the velocity components in the momentum grid points with the QUICK scheme, while the other variables such as turbulence kinetic energy and temperature etc. are predicted in the basic grid points with the HYBRID scheme (Patankar, 1980). At the end of each iteration, the pressure was computed and the velocity components are corrected satisfying the continuity equation, using the Marker and Cell Method (Hirt and Cook, 1972).

The grid spacing in the normal direction (y) was arranged as non-uniform which has high-density grid points near the porous wall according to the distance formulae $\Delta Y_j = \Delta Y_{\min} r^{j-1}$ ($\Delta Y_{\min} = 0.001\,\text{m}, j = 1, 2, \ldots, J_{\text{MAX}}$), where r is the mesh expansion ratio obtained through the iterative solution of $r = [(r-1)(Y_{\text{L}}/\Delta Y_{\min}) + 1]^{1/J_{\text{MAX}}}$. The uniform grid spacing was considered in the x direction with the distance formulae $\Delta X = X_{\text{L}}/I_{\text{MAX}}$ as seen in Figure 2. Based on a grid independence study, a 160×20 grid size was used in the calculating domain. The iterative solution of the discretization equations is considered to be converged when the normalized residuals of the equations are less than a prescribed value of 0.001. All computations were conducted on a PC 600 MHz-Pentium III computer.

Results and discussion

The problem analyzed corresponds to a Reynolds number ($\text{Re} = U_\infty X_{\text{L}}/\nu$) of 4×10^5 for air at a temperature as high as 100°C to allow the developing of the turbulent boundary layer. As is known well, in the boundary layer on a flat plate without injection and suction, transition from laminar to turbulent flow occurs at a critical level of Reynolds number of 3.5×10^5 to 10^6 (Schlichting, 1979) depending on the turbulence intensity (Tu) of the free stream, i.e. it was of the order of 0.01 which was used as an inlet parameter in this study. The problem considered here was investigated computationally by Bellettre *et al.* (1999) for 0.1 m/s of injection velocity in the normal direction. The horizontal velocity and temperature profiles before injection and in the injection region are calculated and compared to the experimental data given by Bellettre *et al.* (1999) (Figures 3 and 4). Comparison of the results for horizontal velocity and temperature with the experimental data showed a good agreement and this agreement encouraged the author to study on tangential transpiration with the methods used in this study.

The numerical results of tangential transpiration for different angles of injection and suction at $x = 1.56\,\text{m}$ are seen in Figures 5-12. It is noticed from these figures that the velocity and thermal fields of the flow field are substantially influenced from the angles of injection, while the flow field parameters are invariable with the variation of angle in the case of suction. It should also be noticed that the effects of the angles of injection between 1 and 90° are similar to the angles of injection between 90 and 180°.

Temperature contours plotted in Figures 13 and 14 give information about the temperature gradients and also heat transfer between the air and the wall. It can be seen clearly that the thermal boundary layer gradients tend to be steeper as the angle of injection approaches 1 and 180°, while the injection angle of 90° causes the less steep thermal boundary layer gradients. This behavior also indicates that

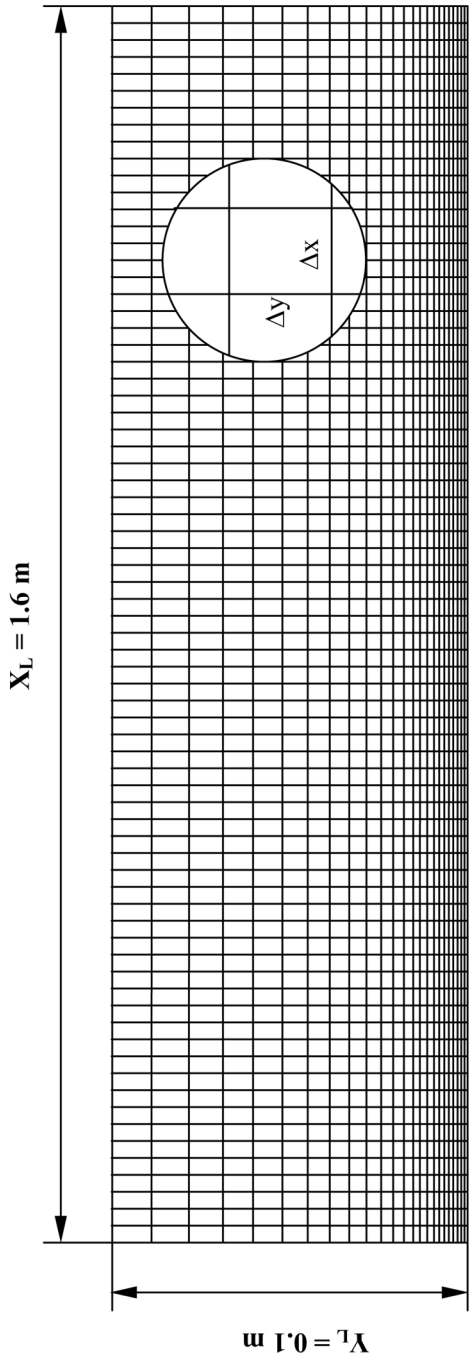

Figure 2.
Grid arrangement

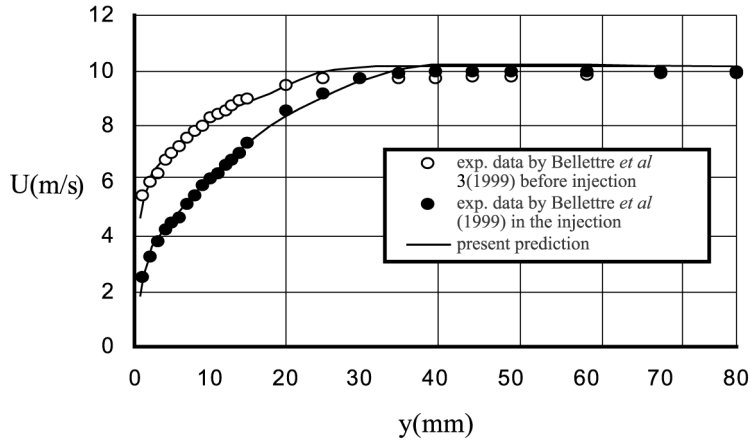

Figure 3.
Comparison of the mean horizontal velocity profiles before ($x = 1.25$ m) and in the injection region ($x = 1.56$ m) with the experimental data

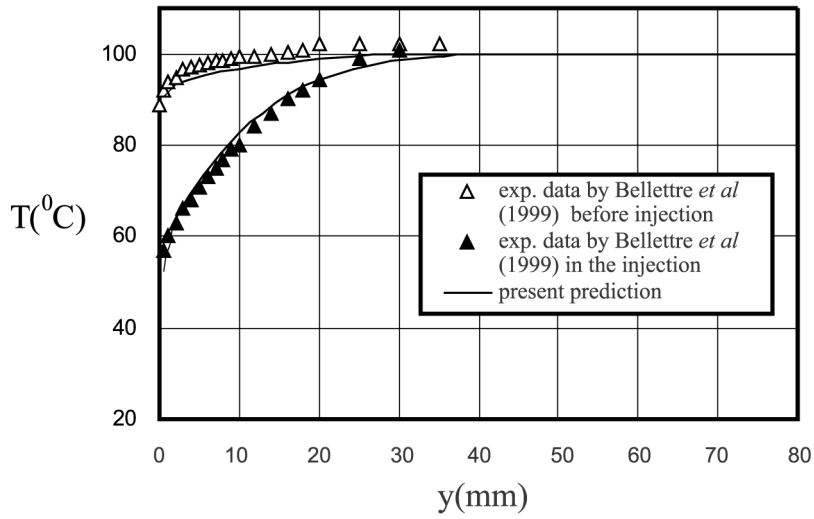

Figure 4.
Comparison of the mean temperature profiles before ($x = 1.25$ m) and in the injection region ($x = 1.56$ m) with the experimental data

the convective heat transfer from hot streaming air to colder wall decreases to its minimum value at the injection with 90°. Temperature contours for the cases of suction indicate clearly that the thermal attribution of the flow field is independent of the angle of suction.

The effects of the angle of the injection and suction on local friction coefficient, is defined as

$$C_f = \frac{2U_\tau^2}{U_\infty} \tag{23}$$

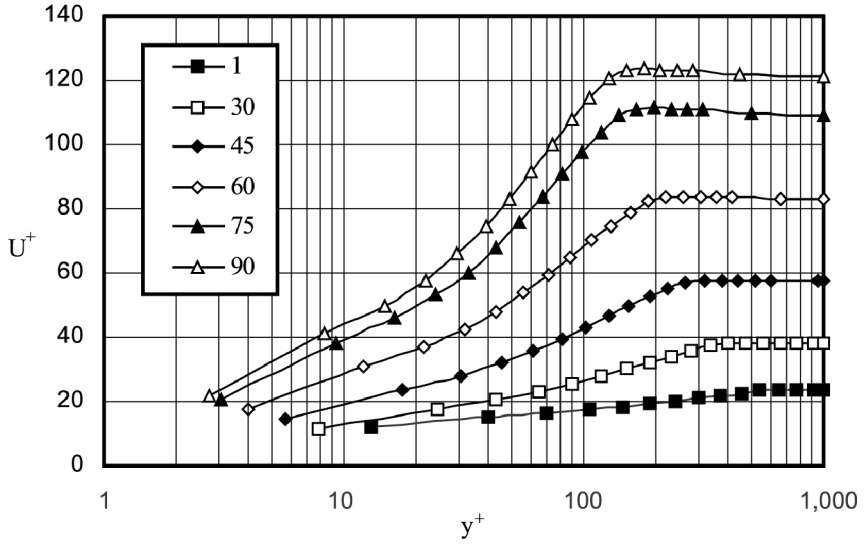

Figure 5.
Normalized mean horizontal velocity profiles at angles between 1 and 90° for $V_w = 0.1$ m/s

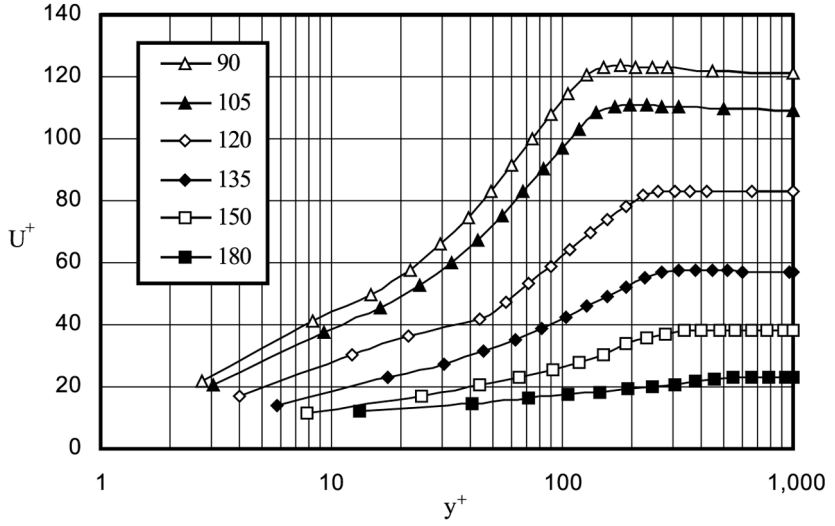

Figure 6.
Normalized mean horizontal velocity profiles at angles between 90 and 180° for $V_w = 0.1$ m/s

are shown in Figures 15 and 16. It can be seen that along the porous wall the local friction coefficient is substantially decreased with increasing angle of injection, while it is slightly increased with increasing angle of suction. It should also be mentioned here that the effect of the angles less than 45° on the local friction coefficient variation is more considerable than the angles greater than 45° in the case of injection. In the case of suction with 1°, the lowest local friction coefficient is relatively obtained.

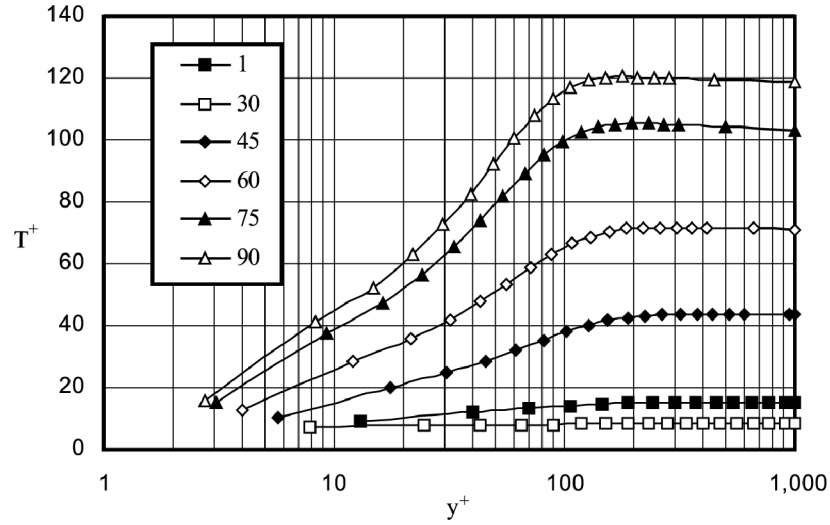

Figure 7.
Normalized mean temperature profiles at angles between 1 and 90° for $V_w = 0.1$ m/s

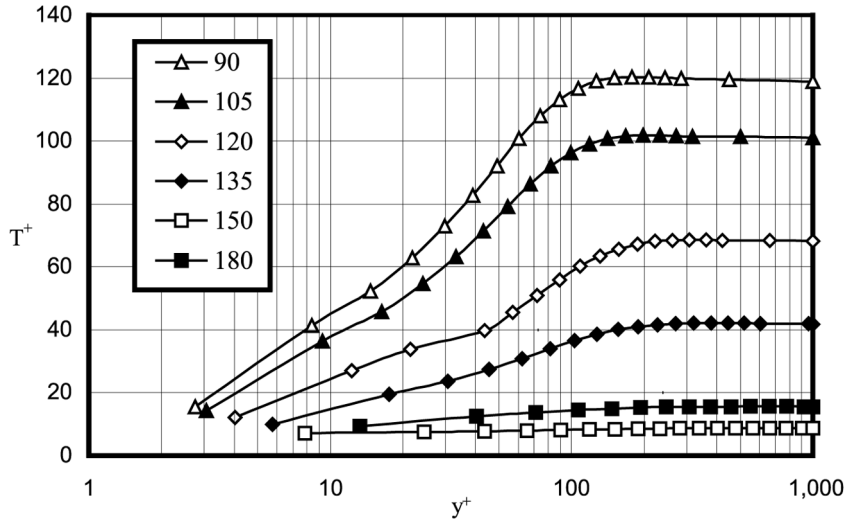

Figure 8.
Normalized mean temperature profiles at angles between 90 and 180° for $V_w = 0.1$ m/s

Regarding the fact that the near-wall heat transfer depends on the thermal boundary layer thickness, the importance of the effects of transpiration application on near-wall heat transfer may be seen. Figure 17 shows that the rate of thermal boundary layer thickness growth in the downstream direction increases as the angle of injection increases. As is seen, while the thermal boundary layer thickness growth significantly depends on the angle of injection for the values between 1 and 45°, the effects of the angles from 45 to 90° on the thermal boundary layer thickness growth can be regarded

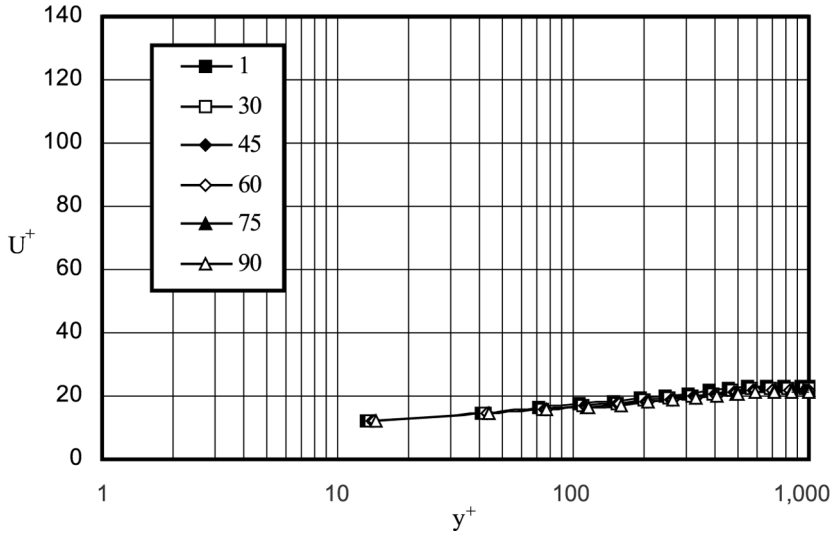

Figure 9.
Normalized mean horizontal velocity profiles at angles between 1 and 90° for $V_w = -0.01$ m/s

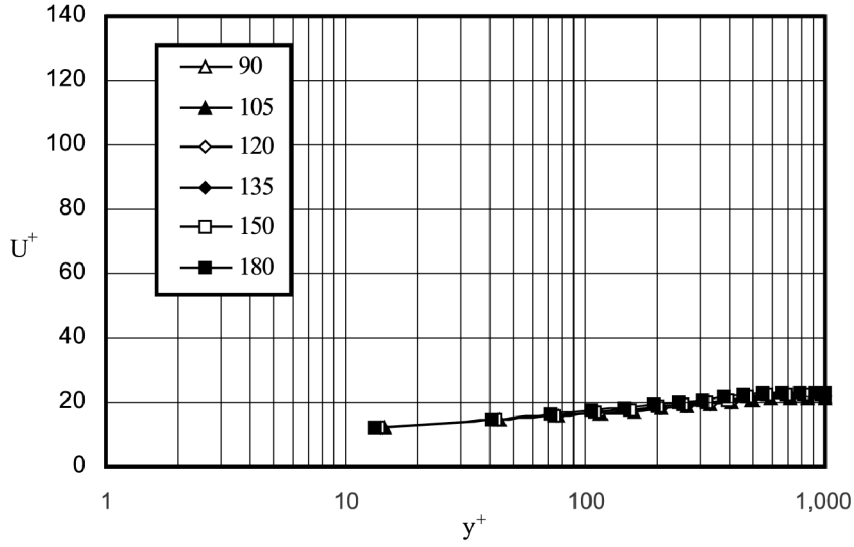

Figure 10.
Normalized mean horizontal velocity profiles at angles of between 90 and 180° for $V_w = -0.01$ m/s

as weak. The effect of the tangential suction through the porous wall on the growth of the thermal boundary layer thickness is also seen in Figure 18.

Conclusions

The flow field with heat transfer and tangential transpiration were predicted by the standard k-ε turbulence model. The results of the normal transpiration, with

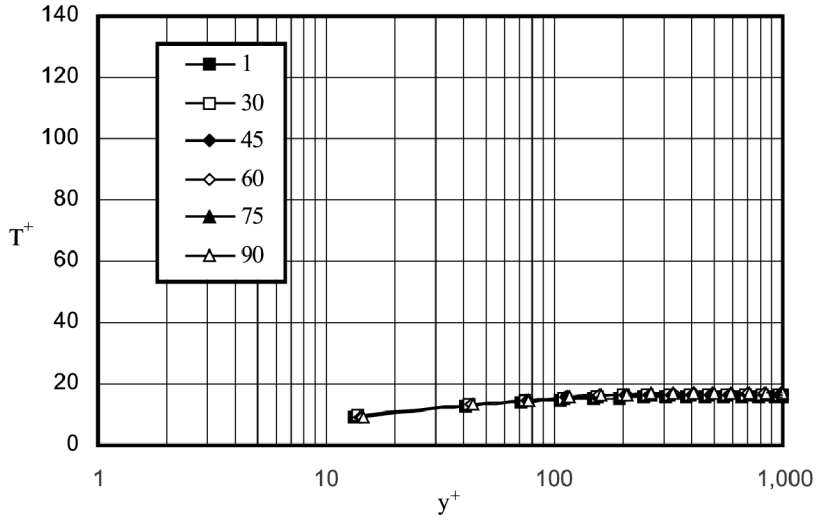

Figure 11.
Normalized mean temperature profiles at angles between 1 and 90 for $V_w = -0.01$ m/s

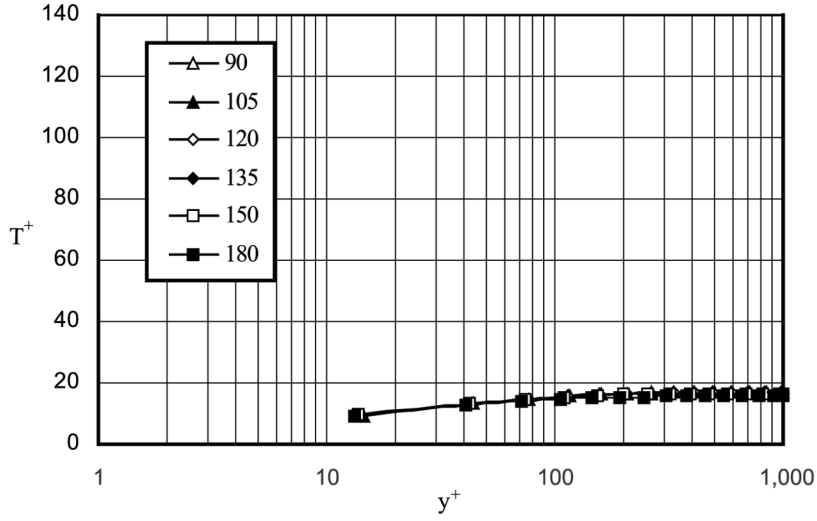

Figure 12.
Normalized mean temperature profiles at angles between 90 and 180° for $V_w = -0.01$ m/s

the modified wall functions including the effects of transpiration, are validated comparing with the experimental measurements. It is concluded that the tangential injection on normal direction causes the lowest drag and also the highest thermal boundary layer thickness which provides the thermal protection, while the suction with the angle of 1° causes the highest heat transfer in conjunction with the lowest drag.

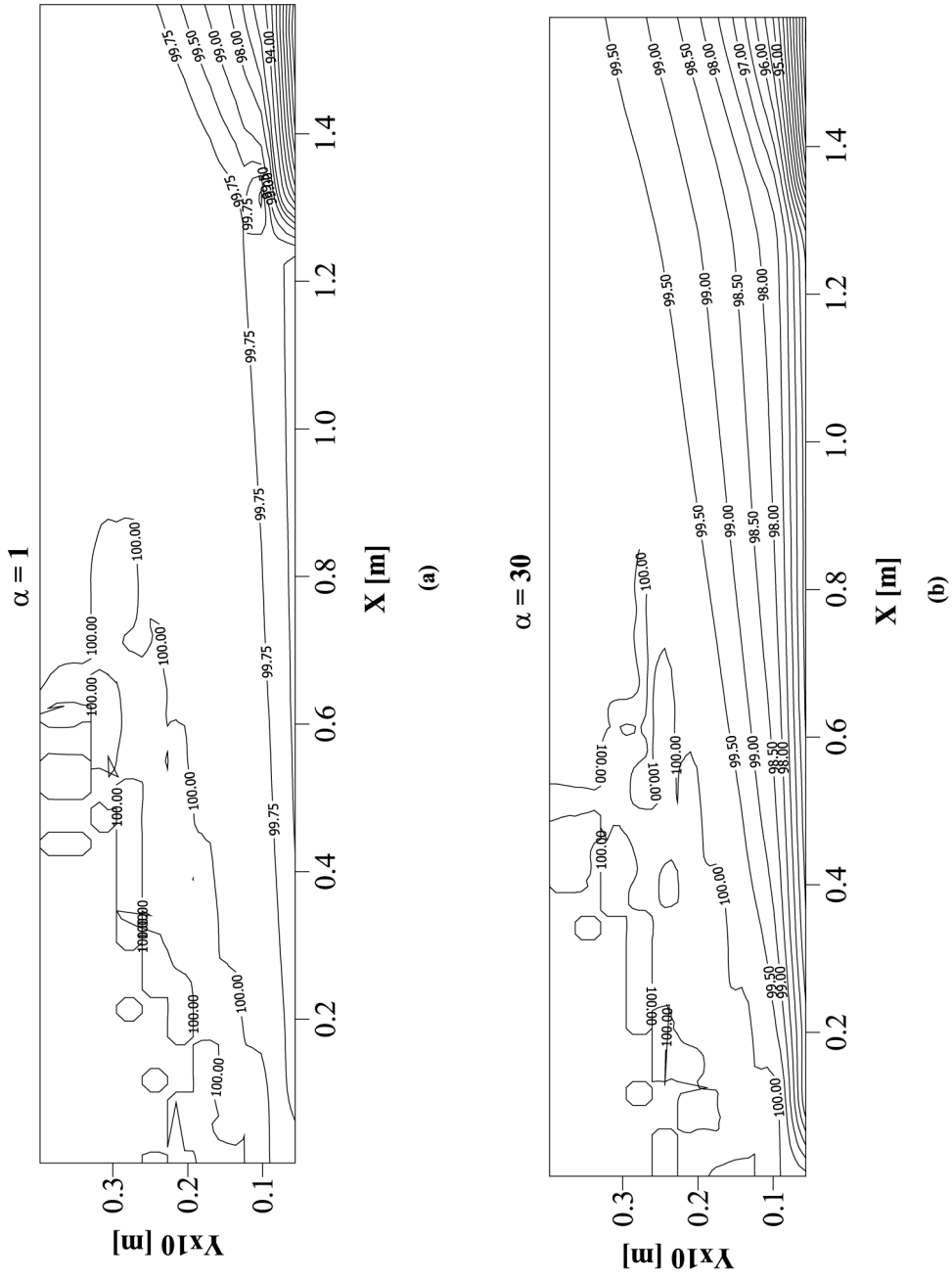

Figure 13.
Contour maps of the temperature at different angles of injection for $V_w = 0.1$ m/s

(Continued)

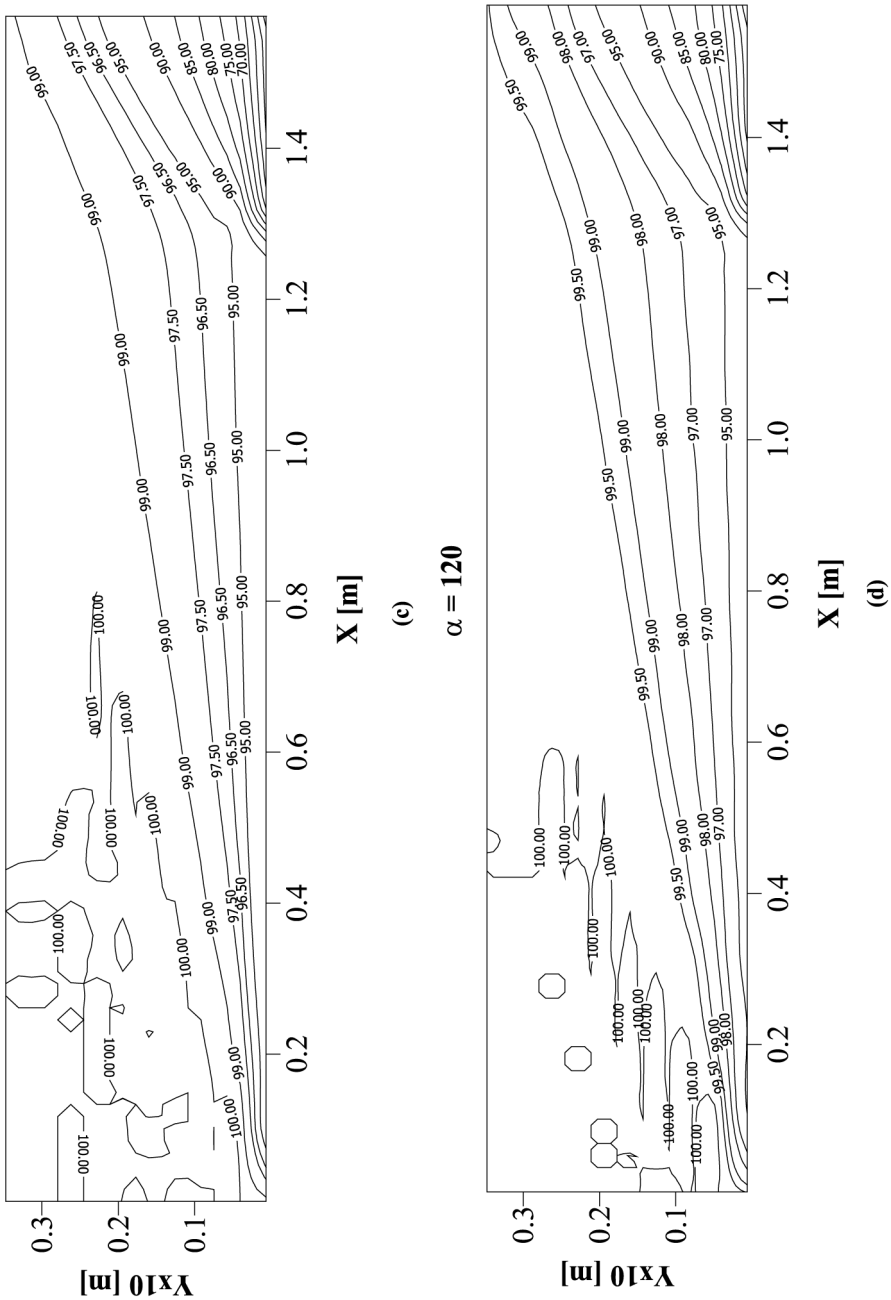

(Continued)

Figure 13.

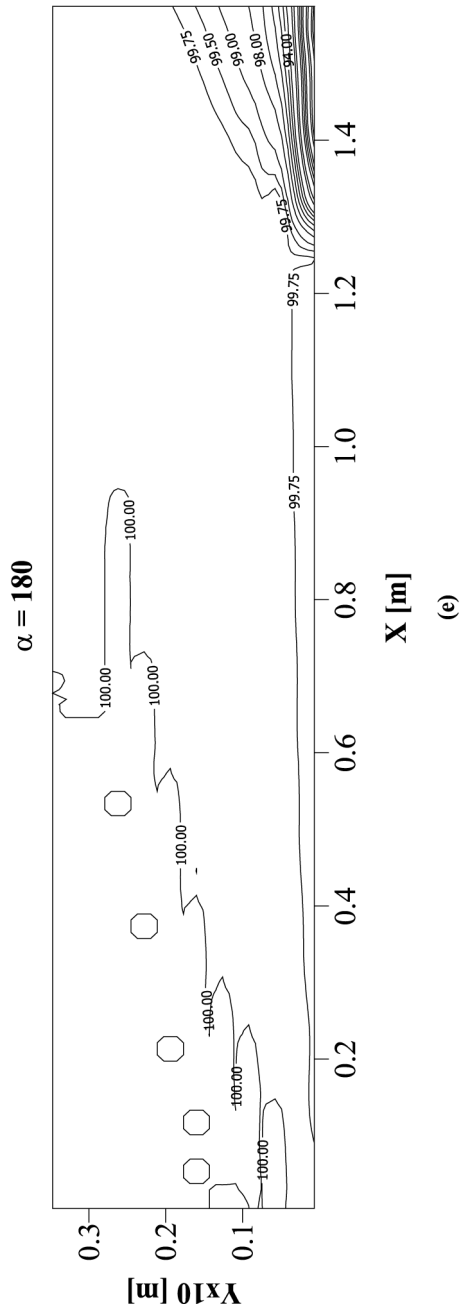
α = 180
Yx10 [m]
X [m]
(e)
0.1
0.2
0.3
0.2
0.4
0.6
0.8
1.0
1.2
1.4
99.75
99.50
99.00
98.00
94.00
100.00

Figure 13.

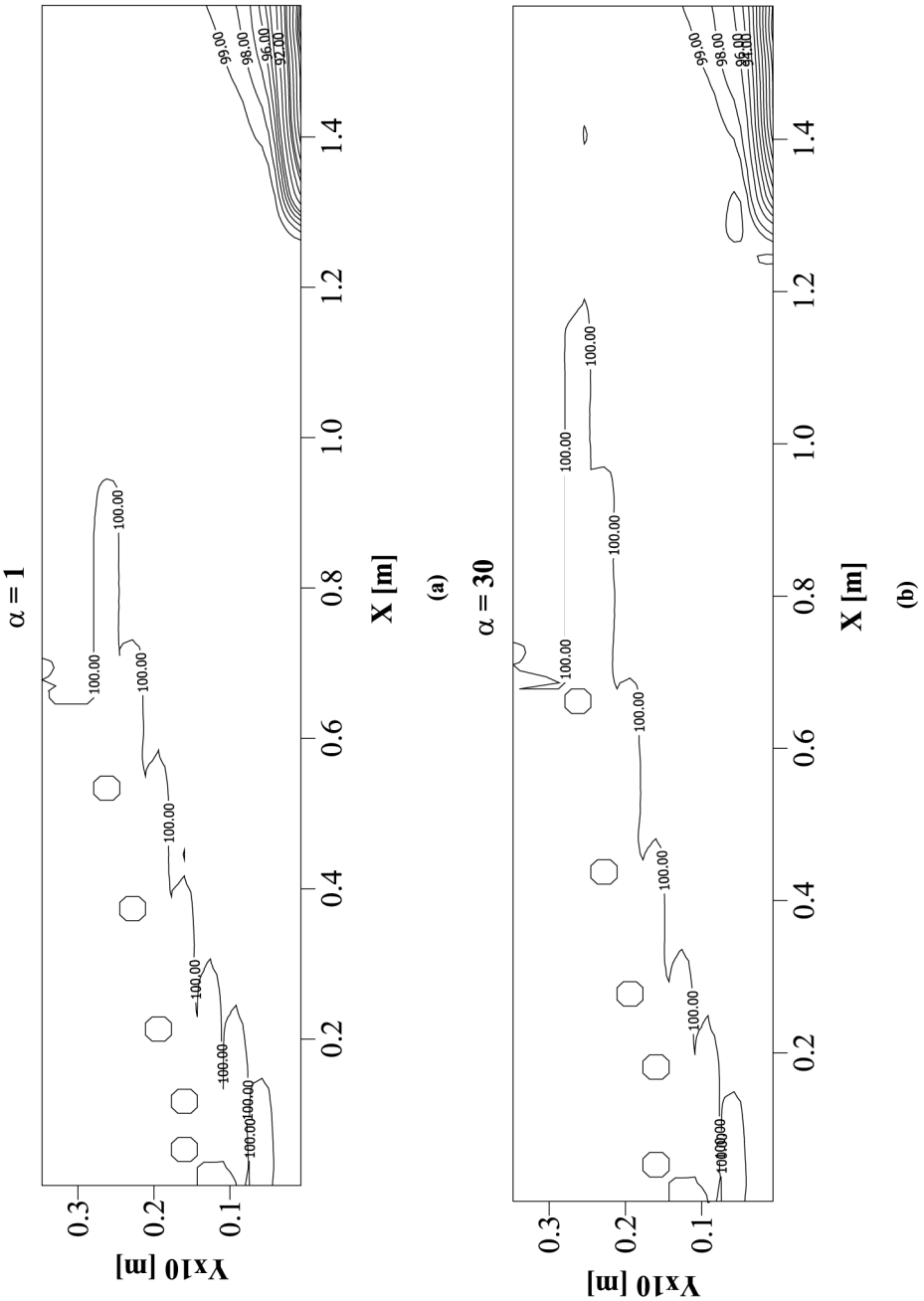

(Continued)

Figure 14.
Contour maps of the temperature at different angles of suction for $V_w = -0.01$ m/s

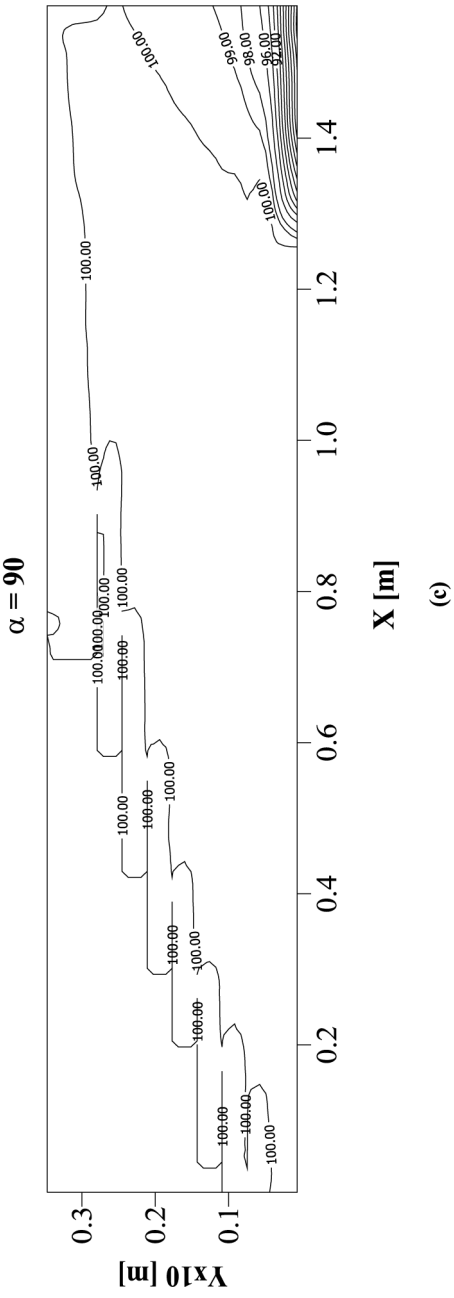

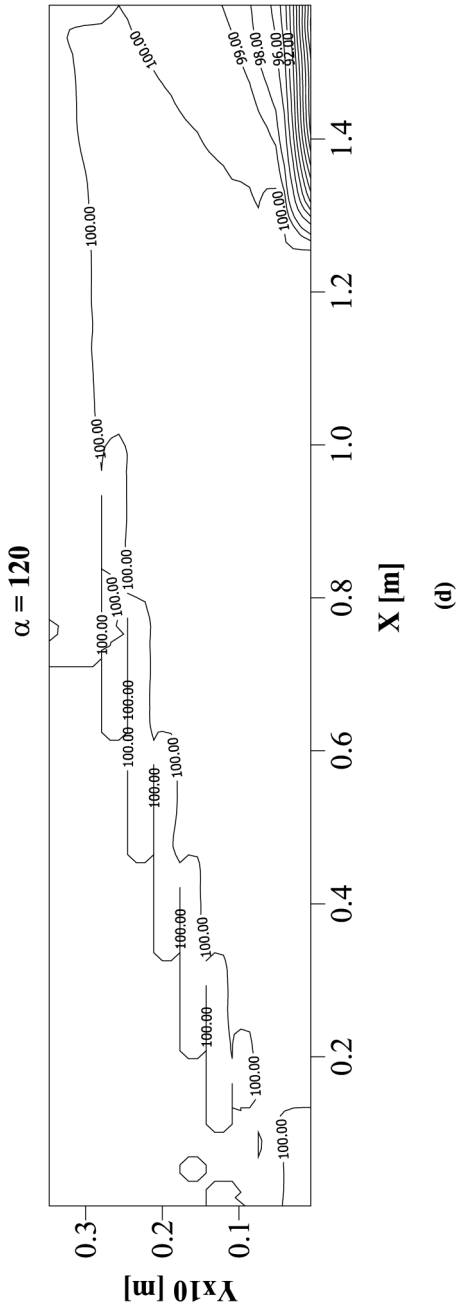

(Continued)

Figure 14.

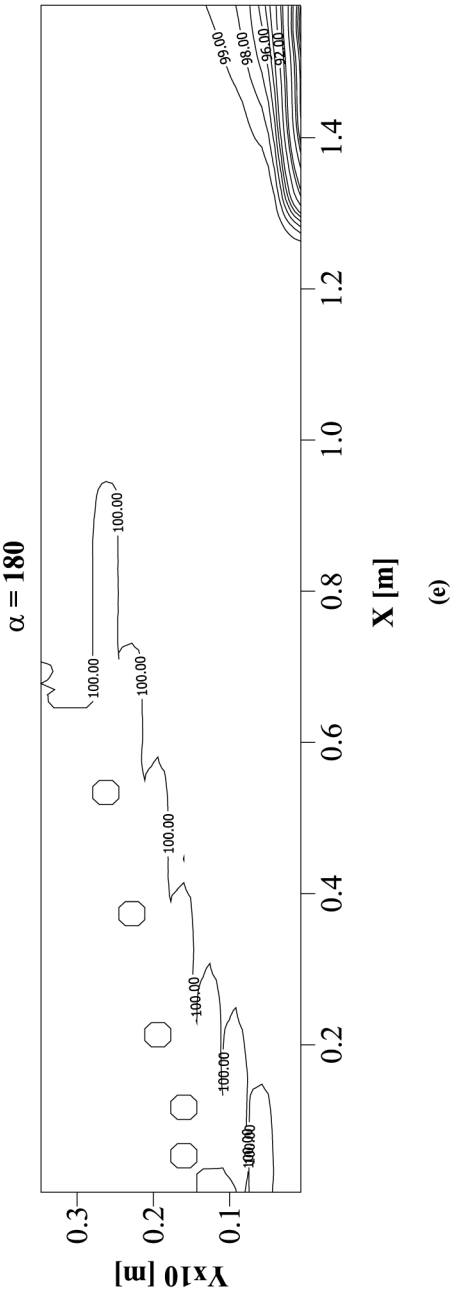
α = 180
Yx10 [m]
X [m]
(e)
0.1
0.2
0.3
0.2
0.4
0.6
0.8
1.0
1.2
1.4
100.00
99.00
98.00
96.00
97.00

Figure 14.

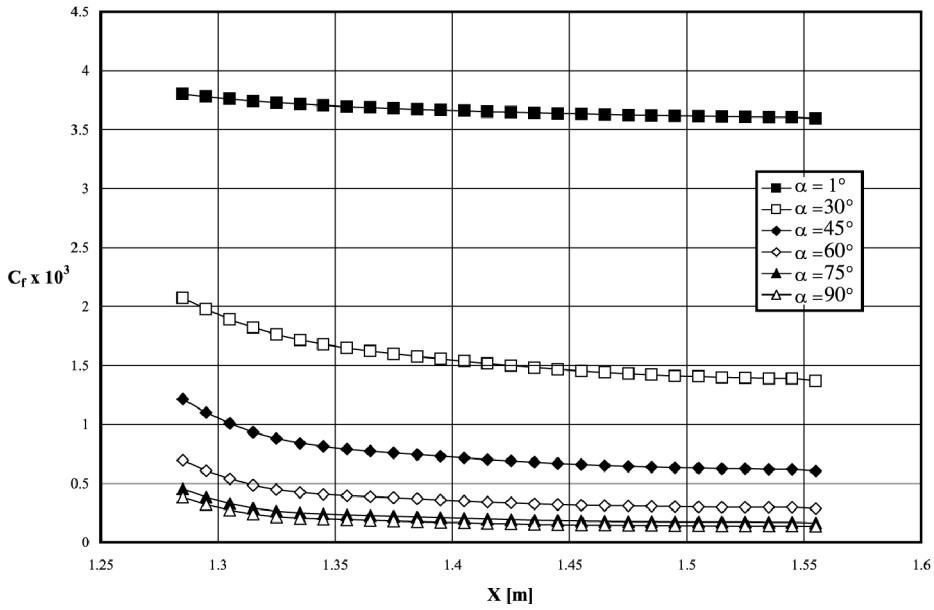

Figure 15.
Local friction coefficient along the porous wall at different angles of injection for $V_w = 0.1$ m/s

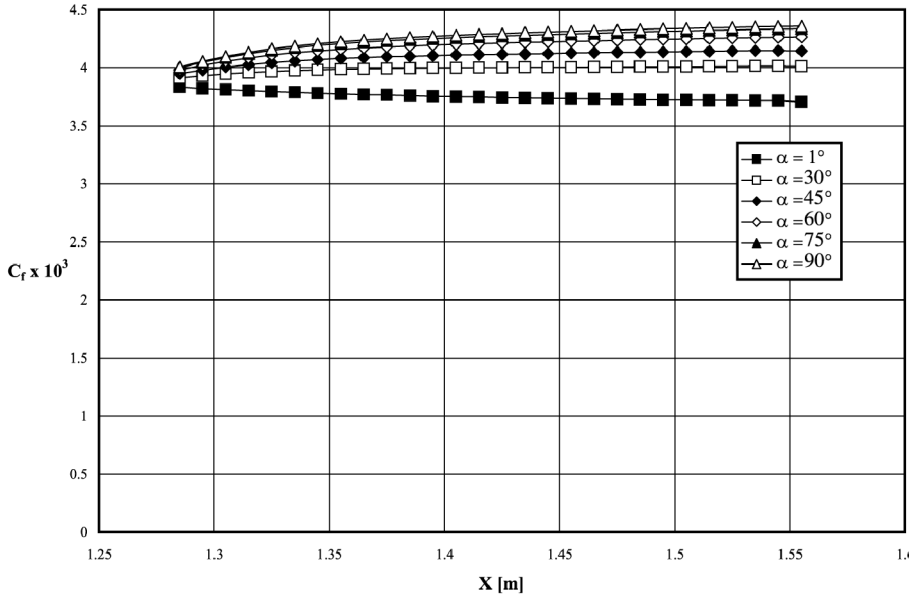

Figure 16.
Local friction coefficient along the porous wall at different angles of suction for $V_w = -0.01$ m/s

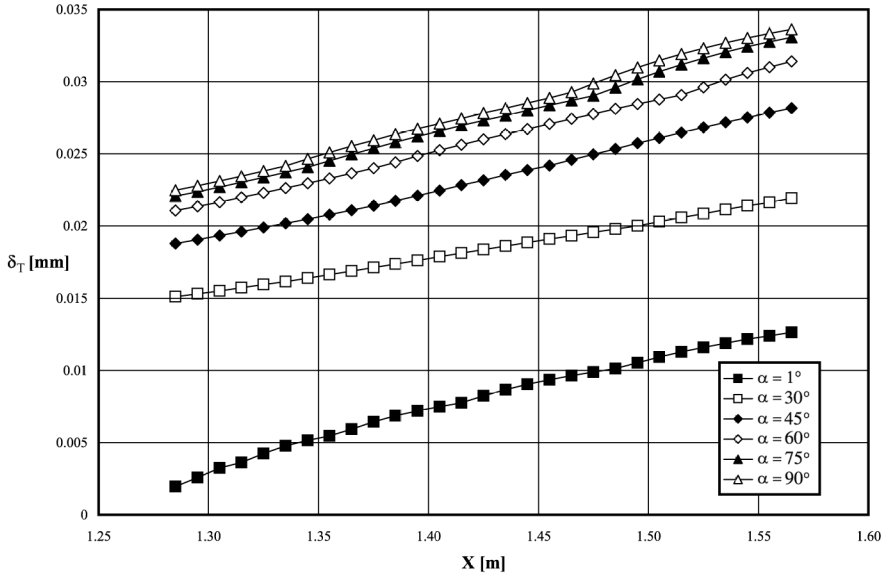

Figure 17.
Thermal boundary layer thickness along the porous wall at different angles of injection for $V_w = 0.1$ m/s

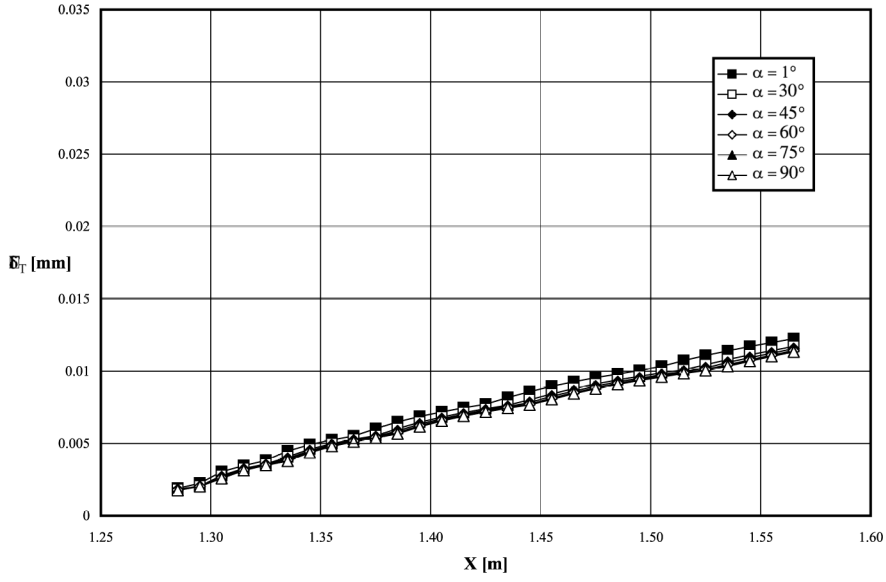

Figure 18.
Thermal boundary layer thickness along the porous wall at different angles of suction for $V_w = -0.01$ m/s

References

Antonia, R.A. and Fulachier, L. (1989), "Topology of a turbulent boundary layer with and without wall suction", *Journal of Fluid Mechanics*, Vol. 198, pp. 429-51.

Antonia, R.A. and Kim, J. (1991), "Turbulent Prandtl number in the near-wall region of a turbulent channel flow", *International Journal of Heat and Mass Transfer*, Vol. 34 No. 7, pp. 1905-8.

Antonia, R.A. and Zhu, Y. (1995), "Effect of concentrated wall suction on a turbulent boundary layer", *Physics of Fluids*, Vol. 7 No. 10, pp. 2465-74.

Avelino, M.R., Su, J. and Silva Freire, A.P. (1999), "An analytical near wall solution for the k-ε model for transpired boundary layer flows", *International Journal of Heat and Mass Transfer*, Vol. 42, pp. 3085-96.

Bellettre, J., Bataille, F. and Lallemand, A. (1999), "A new approach for the study of turbulent boundary layers with blowing", *International Journal of Heat and Mass Transfer*, Vol. 42, pp. 2905-20.

Çuhadaroğlu, B. (2001), "Numerical analysis of the effects of tangential transpiration on the boundary layer characteristics", *International Journal of Numerical Methods for Heat and Fluid Flow*, Vol. 11 No. 8, pp. 793-806.

Djenidi, L. and Antonia, R.A. (2001), "Calculation of the effect of concentrated wall suction on a turbulent boundary layer using a second-order moment closure", *International Journal of Heat and Fluid Flow*, Vol. 22, pp. 487-94.

Hirt, C.W. and Cook, J.L. (1972), "Calculating three-dimensional flows around structures and over rough terrain", *Journal of Computational Physics*, Vol. 10, pp. 324-40.

Hwang, C.B. and Lin, C.A. (2000), "Low Reynolds number k-ε modelling of flows with transpiration", *International Journal for Numerical Methods in Fluids*, Vol. 32, pp. 495-514.

Kays, W.M. and Crawford, M.E. (1980), *Convective Heat and Mass Transfer*, McGraw-Hill, New York, NY.

Lai, Y.G. and So, R.M.C. (1990), "Near-wall modeling of turbulent heat fluxes", *International Journal of Heat and Mass Transfer*, Vol. 33 No. 7, pp. 1429-40.

Patankar, S.V. (1980), *Numerical Heat Transfer and Fluid Flow*, McGraw-Hill, New York, NY.

Schetz, J.A. and Nerney, B. (1977), "Turbulent boundary layer with injection and surface roughness", *AIAA Journal*, Vol. 15 No. 9, pp. 1288-93.

Schlichting, H. (1979), *Boundary-Layer Theory*, McGraw-Hill, New York, NY.

Silva Freire, A.P. (1988), "An asymptotic solution for transpired incompressible turbulent boundary layers", *International Journal of Heat and Mass Transfer*, Vol. 31 No. 5, pp. 1011-21.

Silva Freire, A.P., Cruz, D.O.A. and Pellegrini, C.C. (1995), "Velocity and temperature distributions in compressible turbulent boundary layers with heat and mass transfer", *International Journal of Heat and Mass Transfer*, Vol. 38 No. 13, pp. 2507-15.

Simpson, R.L. (1970), "Characteristics of turbulent boundary layers at low Reynolds numbers with and without transpiration", *Journal of Fluid Mechanics*, Vol. 42 No. 4, pp. 769-802.

So, R.M.C., Sommer, T.P. and Zhao, C.Y. (2000), "Effects of near-wall Reynolds-stress modeling on the calculation of the turbulent thermal field", *International Journal of Heat and Fluid Flow*, Vol. 21, pp. 164-75.

Sucec, J. and Oljaca, M. (1995), "Calculation of turbulent boundary layers with transpiration and pressure gradient effects", *International Journal of Heat and Mass Transfer*, Vol. 38 No. 15, pp. 2855-62.

Yang, J.T., Tsai, B.B. and Tsai, G.L. (1994), "Separated-reattaching flow over a backstep with uniform normal mass bleed", *ASME Journal of Fluids Engineering*, Vol. 116, pp. 29-35.